Mechanobiology in Medicine 3 (2025) 100111

Contents lists available at ScienceDirect

Mechanobiology in Medicine

journal homepage: www.sciencedirect.com/journal/mechanobiology-in-medicine

Full Length Article

Matrix stiffness and viscoelasticity influence human mesenchymal stem cell immunomodulation

Sara J. Olsen [a], Rose E. Leader [b], Abigail L. Mortimer [a], Bethany Almeida [a,*]

[a] Department of Chemical and Biomolecular Engineering, Clarkson University, Potsdam, NY 13699, USA
[b] Department of Mechanical and Aerospace Engineering, Clarkson University, Potsdam, NY 13699, USA

ARTICLE INFO

Keywords:
Human mesenchymal stem cell
Immunomodulation
Matrix stiffness
Matrix viscoelasticity
Biomaterials

ABSTRACT

Human mesenchymal stem cells (hMSCs) have immense wound healing potential due to their immunomodulatory behavior. To control this behavior and reduce heterogeneity, researchers look to biomaterials, as matrix stiffness and viscoelasticity have been shown to control hMSC immunomodulation. However, the understanding of the effects of these biophysical cues on hMSC immunomodulation remains limited; a broad study investigating the potentially synergistic effects of matrix stiffness and viscoelasticity on hMSC immunomodulation is needed in order to support future work developing biomaterials for hMSC wound healing applications. We developed polyacrylamide (PAAm) gels with varying matrix stiffnesses with or without a viscoelastic element and explored the effects of these on hMSC-matrix interactions and immunomodulatory cytokine expression in both a normal growth media and an immunomodulatory growth media mimetic of a chronic, non-healing wound. Expression of IL-10, VEGF, and PGE_2 were upregulated in immunomodulatory growth media over normal growth media, demonstrating the synergistic effects of biochemical signaling on hMSC immunomodulatory behavior. In addition, the addition of a viscoelastic element had both inhibitory and accentuating effects based on the cytokine and biochemical signaling in the cell culture media. Overall, this study provides a broad perspective on the immunomodulatory behavior of hMSCs due to stiffness and viscoelasticity.

1. Introduction

Human mesenchymal stem cells (hMSCs) are an attractive cell source to treat a myriad of human diseases and injuries, as evidenced by their use in >400 clinical trials to date (clinicaltrials.gov).[1–5] They possess the innate capability to differentiate into a variety of adult cell types including bone, cartilage, and fat, which makes them an excellent treatment method for bone and cartilage tissue engineering. Perhaps even more interesting and therapeutically relevant, however, is the fact that hMSCs also play important immunomodulatory roles in the wound healing process, such as in stimulating macrophage M1-M2 transition,[2] inhibiting T-cell activation,[3–5] and stimulating release of anti-inflammatory cytokines.[2,6] For example, prior literature has demonstrated that hMSCs modulate the immune response by secreting proinflammatory cytokines, such as tumor necrosis factor (TNF-α), interferon-λ (IFN-λ), interleukin-1α (IL-1α), and IL-1β.[7] When administered to an active immune response, hMSCs decrease the secretion of IFN-λ and TNF-α and increase the production of the anti-inflammatory cytokines IL-4 and IL-10 in the wound.[8] This immunomodulatory potential makes hMSCs particularly useful in the treatment of chronic non-healing wounds, which are full-thickness lesions that can result in cellulitis, infective venous eczema, gangrene, hemorrhage, and even lower-extremity amputations.[9,10]

However, hMSC therapies have yet to move beyond clinical trials and enter the market. This is due to several limitations including low viability, poor engraftment, and the risk of eliciting an immune response after injection at the site of the wound, which reduces their therapeutic potential.[11–16] Additionally, hMSCs tend to have heterogeneous behaviors due to variability in donor, age, and tissue source.[17,18]

How can we overcome these barriers and enhance the therapeutic potential of hMSCs for wound healing applications? Previous literature has demonstrated that hMSCs have a mechanical memory, allowing hMSCs to recall past physical signals in such a way that allows researchers to "prime" the cells towards specific lineages.[19] HMSCs are also known to be highly mechanosensitive, where their phenotype changes in response to the physical cues around them.[20–22] In particular, matrix stiffness and viscoelasticity have been demonstrated to have a significant effect on modulating hMSC fate. In the seminal paper by Engler et al.,

* Corresponding author. 8 Clarkson Ave, Potsdam, NY 13699, USA.
E-mail address: balmeida@clarkson.edu (B. Almeida).

https://doi.org/10.1016/j.mbm.2024.100111
Received 6 August 2024; Received in revised form 2 December 2024; Accepted 2 December 2024
Available online 8 December 2024

hMSCs were shown to differentiate according to the stiffness of their substrate, with hMSCs on soft matrices mimicking the brain undergoing neurogenesis, hMSCs on stiffer matrices mimicking muscle undergoing myogenesis, and hMSCs on rigid matrices mimicking bone undergoing osteogenesis.[23] In addition to substrate elasticity, researchers have looked at the effect of viscoelasticity on hMSC fate, as human tissues are naturally viscoelastic. Chaudhuri et al. found that cell spreading, proliferation, and osteogenic differentiation were all enhanced on hydrogels with faster matrix stress relaxation.[24,25] Since these and other discoveries in the field of hMSC mechanobiology, it has become clear that the physical properties of the substrate onto which hMSCs are cultured can provide the physical cues to tune their phenotype, and various biomaterials have been explored to mimic these physical cues.[26–30]

However, while the effects of substrate stiffness and viscoelasticity on hMSC differentiation have been well explored, our understanding of the mechanisms by which physical cues affect hMSC immunomodulation remains relatively unknown. Although few studies in the literature have examined this, some literature exists: both the Seib[31] and the Van Vliet groups[32] have shown that stiffness and viscoelasticity influence hMSC cytokine secretion, with softer profiles[33] and more viscoelastic[34] substrates leading to enhanced immunomodulatory and angiogenic profiles. Phuagkhaopong et al. investigated the effect of stress relaxation in silk hydrogels and found that an elastic hydrogel activated IL-1β signaling, induced higher glucose and glutamine consumption, and led to higher lactate secretion in hMSCs.[31] Additionally, the Wenzel group has shown that focal adhesion kinase signaling influences the anti-inflammatory function of hMSCs in response to shear forces.[34] A recent study by the Shin group suggests possible mechanisms behind the effects of matrix stiffness on immunomodulation, demonstrating that soft matrices increase clustering of TNF receptors, enhance NF-κB activation and actin polymerization, and regulate mechanosensitive activation of hMSCs by TNFα with lipid rafts[20]. However, Shin's work studied a single aspect of hMSC immunomodulation, monocyte production, and chemotaxis, and investigated only stiffness and not viscoelasticity. Other studies suggest that 3D culture of hMSCs is more important than matrix stiffness and viscoelasticity in expressing key immunomodulatory genes.[35]

These studies clearly demonstrate the impact that biophysical properties have on the immunomodulatory potential of hMSCs. However, there is missing from the literature a comprehensive study that seeks to demonstrate the synergistic relationship between matrix stiffness and viscoelasticity on hMSC immunomodulatory behavior for a range of elastic, storage, and loss moduli. Thus, we seek to investigate the synergistic effects of substrate stiffness and viscoelasticity on hMSC immunomodulatory behavior using highly tunable polyacrylamide (PAAm) gels for a range of biophysical properties. PAAm gels, due to their ease of fabrication and tunability, allow us to precisely mimic the physical properties of the hMSC microenvironment in 2D. The results of this study will contribute to the growing body of knowledge in the field of hMSC mechanobiology, working towards elucidating the mechanisms by which physical cues affect hMSC immunomodulation.

2. Methods and materials

2.1. Materials

Bone marrow-derived hMSCs (black male aged 38) were purchased from Lonza (Hopkinton, MA). Penicillin-streptomycin was purchased from Cytiva (Marlborough, MA). Triton™ X-100, 75 mm glass slides, 60 mm Petri dishes, 1,4-piperazinediethanesulfonic acid (PIPES), potassium hydroxide (KOH), sodium chloride (NaCl), sucrose, magnesium chloride hexahydrate, and mouse anti-human vinculin monoclonal antibody were purchased from Fisher Scientific (Hampton, NH). Rat anti-human interleukin 10 (IL-10) monoclonal antibody was purchased from eBioscience (San Diego, CA). 35 mm Petri dishes were purchased from Corning (Corning, NY). Low glucose (1 g/L) Dulbecco's modified eagle medium with L-glutamine and sodium pyruvate (DMEM), trypsin-EDTA, and fetal bovine serum (FBS) were purchased from Gibco (Grand Island, NY). Alexa Fluor™ 488 phalloidin, LIVE/DEAD™ cell imaging kit, donkey anti-rat IgG Alexa Fluor™ 488 secondary antibody, mouse anti-human interleukin 6 (IL-6) monoclonal antibody, donkey anti-mouse IgG DyLight™ 594 secondary antibody, mouse anti-human vascular endothelial growth factor (VEGF) monoclonal antibody, goat anti-mouse IgM DyLight™ 488 secondary antibody, and goat anti-rabbit IgG Alexa Fluor™ 594 secondary antibody were purchased from Invitrogen (Waltham, MA). Normal goat serum was purchased from MP Biomedicals™ (Irvine, CA). Prostaglandin 2 (PGE_2) rabbit anti-human polyclonal antibody was purchased from Bioss (Woburn, MA). TWEEN® 20, 4′,6-Diamidino-2-phenylindole dihydrochloride (DAPI), ammonium persulfate (APS), 40 % (w/v) acrylamide solution, 2 % (w/v) N,N′-methylenebisacrylamide solution, (3-aminopropyl)triethoxysilane (APES), 25 % glutaraldehyde in H_2O, dichlorodimethylsilane (DCDMS), N,N,N′,N′-tetramethylethylenediamine (TEMED), 4-(2-Hydroxyethyl)piperazine-1-ethane sulfonic acid (HEPES), sodium hydroxide (NaOH), Dulbecco's phosphate-buffered saline (PBS) without calcium or magnesium, sulfosuccinimidyl6-(4′-azido-2′-nitrophenylamino)hexanoate (sulfo-SANPAH), fibronectin from human plasma, animal-component free recombinant interferon-gamma (IFN-γ), and human recombinant animal-free tumor necrosis factor-alpha (TNF-α) protein were purchased from Millipore Sigma (Billerica, MA). Paraformaldehyde was purchased from Electron Microscopy Sciences (Hatfield, PA). 35 mm Petri dishes with 20 mm No. 1.5 coverglass, uncoated were purchased from MatTek (Ashland, Ma). Cell Counting Kit-8 (CCK-8) was purchased from Dojindo Molecular Technologies (Tokyo, Japan). All chemicals were of analytical reagent quality or high-performance liquid chromatography (HPLC) grade. Ultrapure water (18.2 MΩ cm, Millipore Sigma, Billerica, MA) was used in all experiments requiring water.

2.2. Fabrication and characterization of PAAm gels

Three PAAm gels with low, medium, and high stiffness (elastic moduli) were fabricated by polymerizing a branched network of PAAm in 1 × PBS following the protocol by Tse et al.[36] The elastic moduli of these PAAm gels were modified by using different concentrations of acrylamide and bis-acrylamide monomers in 1 × PBS, as shown in Table 1.[36] Following mixture, the pre-gel monomer solution was filtered and degassed to remove any contaminants and dissolved gas. Subsequently, 1 % APS and 0.1 % TEMED were added to initiate polymerization. A 600 µl drop of this initiated pre-gel solution was placed in between an amino-salinized MatTek dish and a chloro-salinized glass slide and allowed to polymerize for 30 min. After polymerization, the chloro-salinized slide was removed, resulting in a thin, flat gel surface bound to the amino-salinized coverslip on the MatTek dish.

To impart a viscoelastic component to these gels, linear acrylamide was incorporated during polymerization of the branched PAAm network.[37] Linear acrylamide was fabricated by polymerization of an acrylamide monomer solution in 1 × PBS with 1 % APS and 0.1 % TEMED at 37 °C for 1 h. The fabrication of viscoelastic PAAm gels

Table 1
Formulation of PAAm gels.

	Low (−)	Low (+)	Med (−)	Med (+)	High (−)	High (+)
% acrylamide	4.00	4.00	5.00	5.00	5.00	5.00
% bis-acrylamide	0.06	0.06	0.15	0.15	0.30	0.30
% linear Acrylamide	0.00	4.00	0.00	4.00	0.00	4.00
Expected modulus (kPa)	1.16 ± 0.54	1.16 ± 0.54	4.47 ± 1.19	4.47 ± 1.19	8.73 ± 0.79	8.73 ± 0.79

Abbreviations: high, high stiffness; low, low stiffness; med, medium stiffness; -, without linear acrylamide; +, with linear acrylamide.

followed the same protocol as the elastic PAAm gels, with 4 % linear acrylamide in 1 × PBS added in place of the normal amount of 1 × PBS in the pre-gel solution (Table 1). Prior to use in cell studies, the PAAm gels were functionalized with 0.2 mg/mL sulfo-SANPAH in 18.2 MΩ MilliQ water, a heterobifunctional protein cross-linker, and allowed to react under 365 nm ultraviolet (UV) light for 10 min. After functionalization, 10 μg/mL of fibronectin in 50 mM HEPES was added to the PAAm gel and incubated overnight at 37 °C in 5 % CO_2 at 95 % humidity, resulting in a fibronectin-coated PAAm gel.

Young's modulus was measured in experimental triplicate using dynamic mechanical analysis (DMA, DMA850, TA Instruments, New Castle, DE) of 15 mm diameter by 3 mm height bulk PAAm gels. To run the measurements, these gels were placed in between two 15 mm parallel plates, incubated at 37 °C for 5 min, and compressed at a rate of 0.25 mm/min until breaking.

Shear stress was measured in experimental triplicate using a rheometer (AR 2000, TA Instruments, New Castle, DE). Bulk PAAm gels were incubated at 37 °C for 5 min until equilibration and exposed to a frequency sweep from 0.05 to 50 Hz controlled at 2 % strain. The loss modulus, G', storage modulus, G", and tanδ from the frequency sweep were reported at 1 rad/s, which is a relevant frequency for cell mechanosensing.[38]

2.3. Evaluating hMSC immunomodulatory potential

2.3.1. Cell culture

HMSCs were expanded in normal growth medium (low-glucose DMEM supplemented with 10 % v/v FBS, 1 % v/v penicillin-streptomycin, and 4 mM L-glutamine) at 37 °C and 5 % CO_2 to ~85 % confluence prior to passaging using trypsin. For all experiments, expanded hMSCs were plated at 5000 cells/cm^2 on the fibronectin-coated PAAm gels and incubated in either normal growth medium or immunomodulatory medium (normal growth medium supplemented with 20 ng/mL IFN-γ and 10 ng/mL TNF-α[39]) and fed every three days. When the immunomodulatory medium was used, it was used for the entire culture time from cell seeding to assessment. All cells for experiments were used at passage 4–6.

2.3.2. Cytocompatibility

To visualize cytocompatibility, a LIVE/DEAD™ assay was performed on hMSC-seeded elastic and viscoelastic PAAm gels in MatTek dishes 1 and 7 days after cell seeding in normal growth medium following the manufacturer's protocol. This staining solution was added to the cells and allowed to incubate for 15 min at room temperature (RT) prior to imaging. Stained cells were imaged on a Ti2E inverted epi-fluorescence microscope (Nikon, Tokyo, Japan) at 488 nm for calcein AM (live cells) and 594 nm for ethidium homodimer-1 (dead cells). To quantify cytocompatibility and cellular metabolic activity, a CCK-8 assay was performed on hMSC-seeded elastic and viscoelastic PAAm gels in MatTek dishes on days 1, 3, 7, 14, and 21 after cell seeding in normal growth medium following the manufacturer's protocol. Briefly, after the designated incubation period for each sample, 100 μL of CCK-8 was added to 1 mL of normal growth media (1.1 mL total volume per MatTek dish), and the cells were incubated for 2 h at 37 °C. Following incubation, the supernatant was removed from the cells and 150 μL of this CCK-8/growth media solution was placed in a non-tissue culture-treated 96-well plate in technical triplicate. 13.6 μL of 0.1 M HCl was added to each well to preserve sample absorbance. Samples were measured at 450 nm using a Plate Reader (SpectraMax® i3x, Molecular Devices, San Jose, CA). Positive controls of protein-coated MatTek dishes seeded with hMSCs but without PAAm gels and negative controls with no cells and no PAAm gels (normal growth media with CCK-8 solution only) were included. The normalized cell viability was calculated using Eq. (1).

$$Cell\ Viability = \frac{\left(Abs\ 450nm_{sample} - Abs\ 450nm_{negative\ control}\right)}{\left(Abs\ 450nm_{positive\ control} - Abs\ 450nm_{negative\ control}\right)}\ x\ 100 \quad \text{Eq. (1)}$$

2.3.3. Morphology

hMSCs were seeded on elastic or viscoelastic PAAm gels and incubated for 1, 3, 7, 14, and 21 days in either a normal growth medium or immunomodulatory growth medium. Following incubation, the cells were fixed with 4 % paraformaldehyde for 15 min, permeabolized with cytoskeletal buffer for 1 min, and blocked with 10 % normal goat serum for 30 min. Samples were washed with 0.01 % 1 × PBS-tween three times each between steps. To visualize focal adhesions, the hMSCs were incubated with 2 μg/ml of a mouse anti-vinculin primary antibody in 1 % normal goat serum overnight at 4 °C and then incubated with 2 μg/ml of a donkey anti-mouse IgG DyLight™ 594 secondary antibody in 1 % normal goat serum for 1 h. The hMSCs were then counterstained with 2 μM DAPI and 1.65 μM phalloidin AF-488 for 5 and 30 min, respectively, to visualize nuclei and F-actin. The stained hMSCs were imaged on a Ti2E inverted microscope (Nikon, Tokyo, Japan) at 360 nm for nuclei, 488 nm for F-actin, and 594 nm for focal adhesions. Images were processed using FIJI is Just ImageJ to form composite overlaid images of each sample. To quantify morphological analysis, we investigated cell area, aspect ratio, circularity, and roundness using ImageJ's shape descriptors function, where the area is the 2D surface area of the cells in squared pixels, aspect ratio is defined as the length of the major axis divided by the length of the minor axis, circularity is defined as how well the overall shape of the object fits to a perfect circle, with a value of 1.0 indicative of a perfect circle, and roundness is circularity normalized to the aspect ratio. To quantify these values, a region of interest was drawn around individual cells across technical and experimental replicates and the single-cell values were recorded. Days 14 and 21 were not quantified due to high confluence. We also quantified vinculin intensity by quantifying the average pixel intensity of the image, which was normalized per cell and background signal was subtracted.

2.3.4. Cytokine expression

To evaluate the immunomodulatory potential of the hMSCs on the PAAm gels, IL-6, IL-10, VEGF, and PGE_2 were investigated by quantifying their expression through immunocytochemistry. Briefly, hMSCs were seeded on the elastic or viscoelastic PAAm gels for 1, 3, 7, 14, and 21 days in either normal growth medium or immunomodulatory growth medium. Following incubation, the cells were fixed with 4 % paraformaldehyde for 15 min, permeabolized with 0.25 % triton X-100 for 10 min, and blocked with 10 % normal goat serum for 30 min. Samples were washed with 0.01 % 1 × PBS-tween three times each between steps. For each cytokine, the hMSCs were incubated with the corresponding primary antibody in 1 % normal goat serum overnight at 4 °C and then incubated with the corresponding secondary antibody in 1 % normal goat serum for 45 min (Supplementary Table S1 details all primary and secondary antibody concentrations). The cells were additionally counterstained with DAPI for 5 min. The stained hMSCs were imaged on a Ti2E inverted microscope (Nikon, Tokyo, Japan) at 360 nm for nuclei, 488 nm for the IL-10 and IL-6 secondary antibodies, and 594 nm for the VEGF and PGE_2 secondary antibodies. To quantify cytokine expression, all samples were measured using the same power intensity and exposure settings, and all metadata was stored in .nd2 files. Fiji is Just ImageJ was used to quantify pixel intensity for each cytokine, which was normalized per cell and background signal was subtracted. Brightness and contrast were not changed prior to quantifying pixel intensity to allow for direct comparisons between samples.

2.4. Statistical analysis

All measurements were performed in a minimum of experimental and technical triplicate and data is presented as mean ± standard deviation unless otherwise stated. Data was normalized as appropriate and the standard deviation was calculated using the rules of propagation of uncertainty. Box plots for Figs. 5–8 demonstrate the range of data, with the whiskers indicative of the lowest and highest value, the box indicating the 25th-75th percentiles, the line indicating the median, and the dot

Table 2
Characterization of PAAm gel properties.

	Low (−)	Low (+)	Med (−)	Med (+)	High (−)	High (+)
E (kPa)	1.44 ± 0.11	1.15 ± 0.08	4.13 ± 0.51	4.99 ± 0.34	8.54 ± 0.55	8.82 ± 0.22
G' (kPa)	144 ± 21.3	233 ± 51.4	299 ± 50.1	276 ± 73.0	647 ± 63.4	479 ± 105
G" (kPa)	36.6 ± 11.6	81.0 ± 29.1	127 ± 40.3	147 ± 38.4	220 ± 34.6	213 ± 9.56
Tanδ	0.251 ± 0.052	0.373 ± 0.209	0.444 ± 0.213	0.551 ± 0.159	0.341 ± 0.055	0.455 ± 0.078

Abbreviations: E, Young's modulus; G′, storage modulus; G″, loss modulus; High, high stiffness; low, low stiffness; med, medium stiffness; -, without linear acrylamide; +, with linear acrylamide.

indicating the mean. Statistical analysis was conducted using one- or two-way analysis of variance (ANOVA) with Tukey–Kramer *post hoc* analysis using GraphPad Prism Version 10.2.3 as appropriate. Data was considered statistically significant for $p < 0.05$ (note: $*p < 0.05$, $**p < 0.01$, $***p < 0.001$, $****p < 0.0001$).

3. Results and discussion

3.1. Polyacrylamide gel fabrication and characterization

Table 2 shows the measured Young's modulus, loss modulus, and storage modulus values for each gel formulation. Comparing the Young's modulus values with the values expected (Table 1) yields strong agreement, demonstrating successful gel fabrication. We confirm statistically significant differences in Young's modulus between low-, medium-, and high-stiffness gels both with and without a viscoelastic element ($p < 0.0001$ for low- to med-, $p < 0.0001$ for low- to high-, and $p < 0.0001$ for med- to high-stiffness without a viscoelastic component and $p < 0.0001$ for low- to med-, $p < 0.0001$ for low- to high-, and $p < 0.0001$ for med- to high-stiffness with a viscoelastic component). In addition, the storage modulus, which relates to the elastic behaviour of materials, increases proportionally with the Young's modulus. Meanwhile, stiffness of the gel does not change between gels with or without a viscoelastic element ($p = 0.900$ for low-stifness gels, $p = 0.089$ for medium-stiffness gels, and $p = 0.916$ for high-stiffness gels). This is as expected, as we do not expect the addition of the linear acrylamide to significantly affect the overall elasticity of the gels.

The loss modulus, related to the viscous behaviour of materials, was not found to be statistically significant between non-viscoelastic and viscoelastic gels for any stiffness, low-, medium-, or high-. This is likely due to the large standard deviations, which were a result of batch-to-batch variability in gel fabrication. The lack of statistical significance continued for Tanδ, a ratio measurement indicative of elastic:viscous components with larger Tanδ suggesting increased viscous components, values. However, although not statistically significant, trends for the low- and medium-stiffness gels appear to be increasing from the non-viscoelastic to viscoelastic PAAm gels. On the contrary, there appears to be no difference in loss modulus for the high-stiffness gels, although these similarly have the trend of an increased Tanδ (albeit not statistically significant). This may be related to the increased concentration of bis-acrylamide in the high stiffness gels (Table 1) yielding a higher chance of the linear acrylamide crosslinking to the acrylamide matrix at its terminal ends.[36] To further investigate potential differences in crosslinking due to the presence of acrylamide and bis-acrylamide concentrations, a very high-stiffness, non-viscoelas tic and viscoelastic PAAm gel were also made, with an expected Young's modulus of ~19.66 kPa (8 % acrylamide, 0.26 % bis-acrylamide, data not shown in Table 1). The measured Young's modulus of these gels was found to be 9.50 ± 0.99, and 20.1 ± 0.94 kPa for the very high-stiffness, non-viscoelastic and viscoelastic PAAm gels, respectively. Interestingly, the very high-stiffness gel did show an increase in Young's modulus when linear acrylamide was added, suggesting that the addition of the linear acrylamide was increasing the number of overall crosslinks in the polymer matrix. Further investigation is needed to dissect this phenomenon. However, as the focus of this study was on the cell effects and there was a trending increase in the Tanδ, we proceeded with these gels. In addition, while the elastic gels remained optically transparent, the viscoelastic gels became opaque, with the degree of opaqueness increasing from low- to medium- to high-stiffness gels (Supplementary Fig. S1).

3.1.1. hMSC-matrix interactions

Prior to investigating the synergistic effects of matrix stiffness and viscoelasticity on cytokine expression, we first investigated the hMSC-matrix interactions. As previously mentioned, hMSCs are mechanosensitive; thus, variations to hMSC-matrix interactions due to matrix stiffness and viscoelasticity may be related to variations in cytokine expression mechanistically.[40] We confirmed that the cells remain viable and proliferative on these gels, with few dead cells present on day 1 (Supplementary Fig. S2).

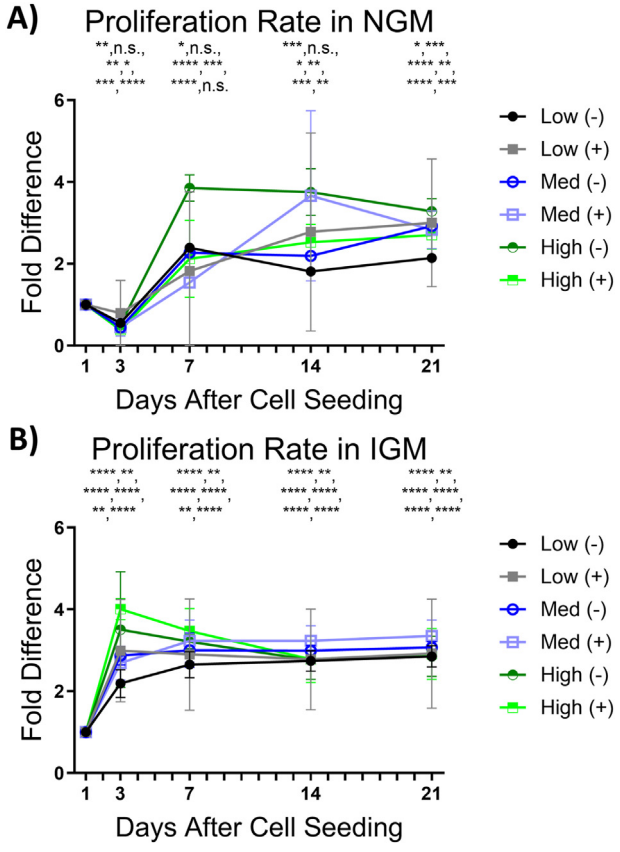

Fig. 1. Proliferation rate with time in A) normal growth medium (NGM) and B) immunomodulatory growth medium (IGM) shown for hMSCs cultured on each polyacrylamide gel measured using a CCK-8 assay 1, 3, 7, 14, and 21 days after initial cell seeding. Statistics are shown on Days 3, 7, 14, and 21 and are all compared to their respective Day 1 time point for each gel type, listed in order as, low (−), low (+), med (−), med (+), high (−), and high (+). Data was considered statistically significant for $p < 0.05$ (Note: $*p < 0.05$, $**p < 0.01$, $***p < 0.001$, $****p < 0.0001$).

In normal growth medium, cells rapidly proliferate on all gel formulations, reaching a 2-fold–4-fold increase in proliferation after 21 days (Fig. 1A). In this study, we normalized the initial cell count at day 1 for each gel type to '1', and the rate of proliferation at each time point is conducted in comparison to a change from this day 1 time point (i.e., a rate of '2' means 100 % proliferation, or a population doubling). Interestingly, proliferation rate was generally highest on the high-stiffness gels and lowest on the low-stiffness gels. For non-viscoelastic gels, the proliferation rate at days 7 and 14 are statistically significant for high-stiffness gels in comparison to low- and medium-stiffness gels, while at day 21, high-stiffness gels are only statistically greater than low-stiffness gels (Supplementary Fig. S3Aii). Viscoelastic gels, on the other hand, have a more consistent proliferation rate between gel stiffnesses (Supplementary Fig. S3Aiii). Supplementary Fig. S3Aiv-vi also depicts differences at each time point for each stiffness gel independent of the other stiffness gels, showing that the low- and medium-stiffness gels had high

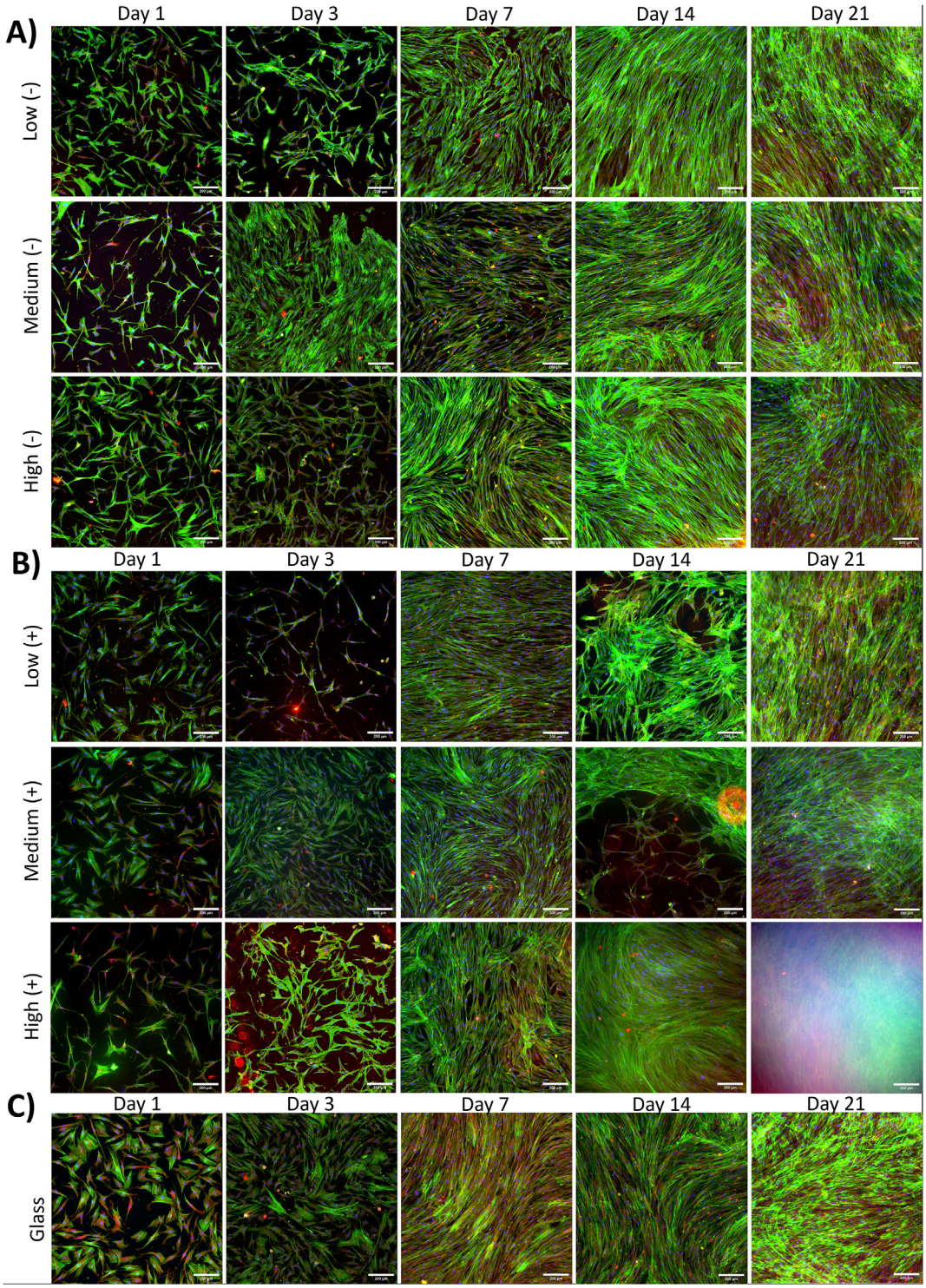

Fig. 2. Morphology of hMSCs cultured on each PAAm gel formulation for 1, 3, 7, 14, and 21 days in normal growth medium. A) Non-viscoelastic gels, B) Viscoelastic gels, and C) Glass. Green = F actin, Blue = nuclei, Red = vinculin, Scale Bar = 200 μm.

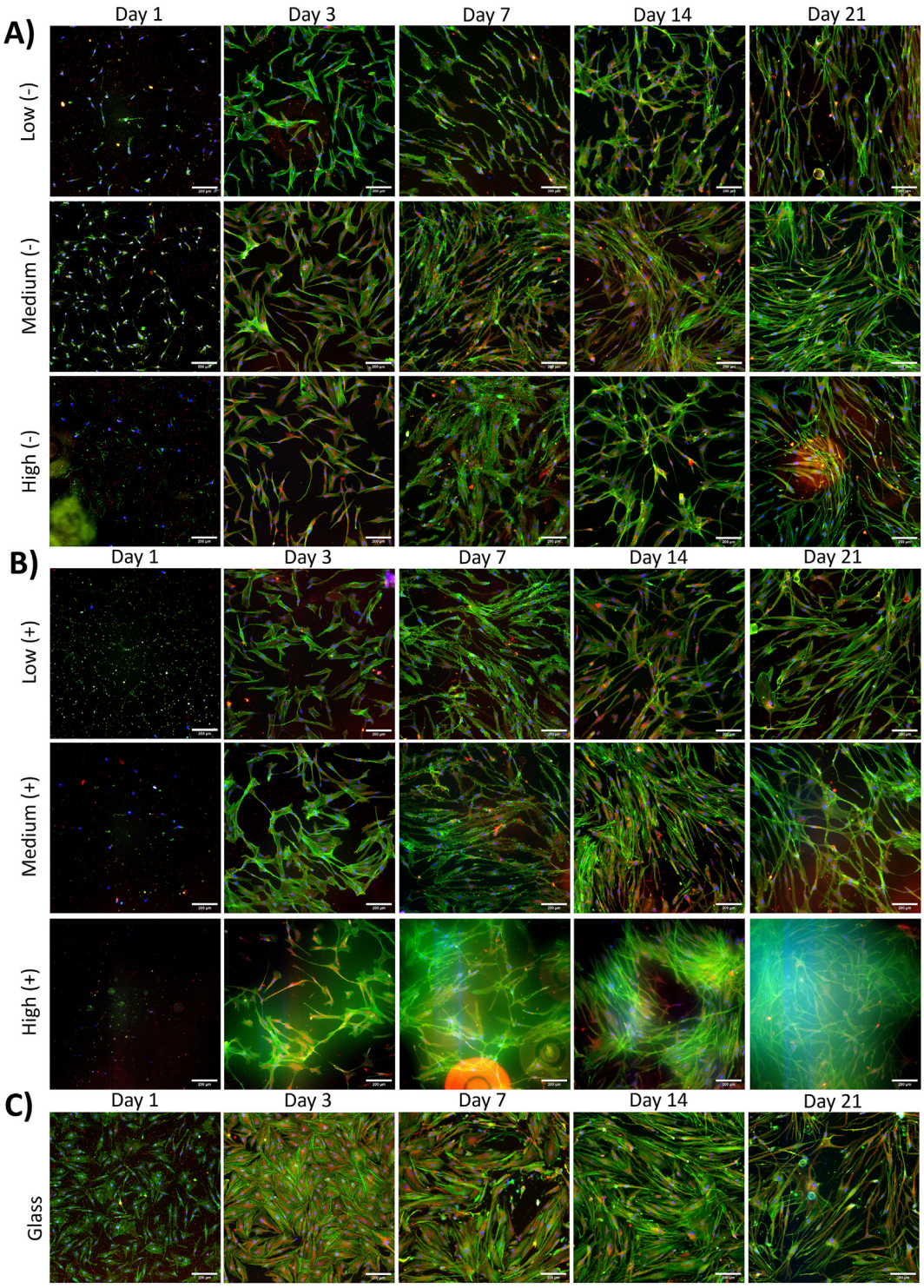

Fig. 3. Morphology of hMSCs cultured on each PAAm gel formulation for 1, 3, 7, 14, and 21 days in immunomodulatory growth medium. A) Non-viscoelastic gels, B) Viscoelastic gels, and C) Glass. Green = F actin, Blue = nuclei, Red = vinculin, Scale Bar = 200 μm.

similarity in proliferation rate for viscoelastic and non-viscoelastic gels, while the high-stiffness, non-viscoelastic gels had statistically significant proliferation in comparison to viscoelastic gels at days 7, 14, and 21.

The effects of the immunomodulatory media attenuated the effects of the gel formulation on cell proliferation rate overall. Interestingly, cells cultured in normal growth media appeared to experience a decline in overall cell number between days 1 and 3 before rapidly proliferating as previously described. However, in immunomodulatory media, the opposite is true, and there is a rapid initial growth from days 1–3 for cells on all gel conditions before this proliferation tapers and plateaus from days 7–21 at around 3-fold increase over day 1 (Fig. 1B). We attribute this to the overall lower number of cells initially on gels in the immunomodulatory media compared to cells initially on gels in the normal growth media. Further, in comparison to cells in normal growth medium, where there were significant differences between gel conditions, there are little-to-no differences between gel stiffnesses for non-viscoelastic and viscoelastic gels (Supplementary Fig. S3Bi-vi) in immunomodulatory media.

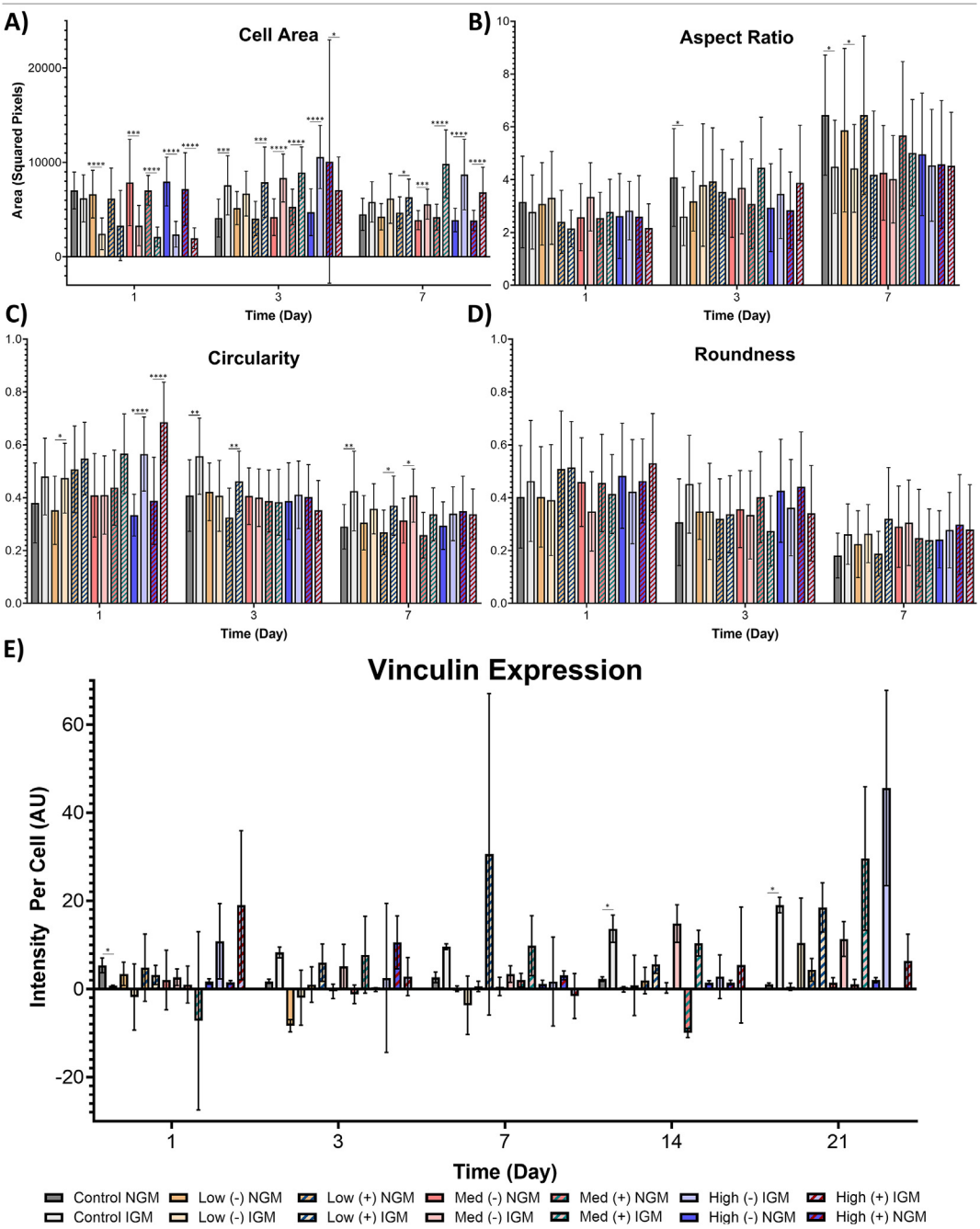

Fig. 4. Morphological analysis of cells in normal growth media vs. immunomodulatory growth media for all gel conditions over time, looking at A) cell area, B) aspect ratio, C) circularity, D) roundness, and E) vinculin expression. Data was considered statistically significant for $p < 0.05$ (Note: *$p < 0.05$, **$p < 0.01$, ***$p < 0.001$, ****$p < 0.0001$).

As cell shape is known to directly relate to cell behaviour for hMSCs,[41] we also sought to understand the effects of the different gel formulations in the two media conditions (Figs. 2 and 3 for normal growth media and immunomodulatory growth media, respectively) on hMSC morphology. Of note, due to the high opaqueness of the high-stiffness, viscoelastic gels, it can be challenging to visualize cells with fluorescence due to the resulting background signal. To aid in viewing the cells, Supplementary Fig. S4 shows the cells at day 21 cultured on high-stiffness, viscoelastic gels in normal growth media and immunomodulatory growth media for all imaging channels.

Prior literature has shown that culture on lower-stiffness, higher-viscoelasticity gels typically result in smaller hMSCs with more rounded morphologies, while culture on higher-stiffness, non-viscoelastic gels typically result in larger cells with greater elongations and protrusions.[23]

Interestingly, culture in immunomodulatory growth media vs. normal growth media also had an effect on the overall cellular morphology, and this effect appeared to dominate over any morphological changes due to stiffness or viscoelasticity. For example, cell area was found to be smaller on cells cultured in immunomodulatory growth media at day 1, regardless of the gel condition (Fig. 4A). In addition, there are fewer cells on day 1, indicating that many cells did not survive adhesion due to the combined presence of the inflammatory molecules and the gels. It is unlikely that the lower adhesion is simply due to the inflammatory molecules as we saw high initial cell adhesion on the control sample. However, this trend reverses at days 3 and 7, with statistically significant increases in cell areas for cells cultured in immunomodulatory growth media

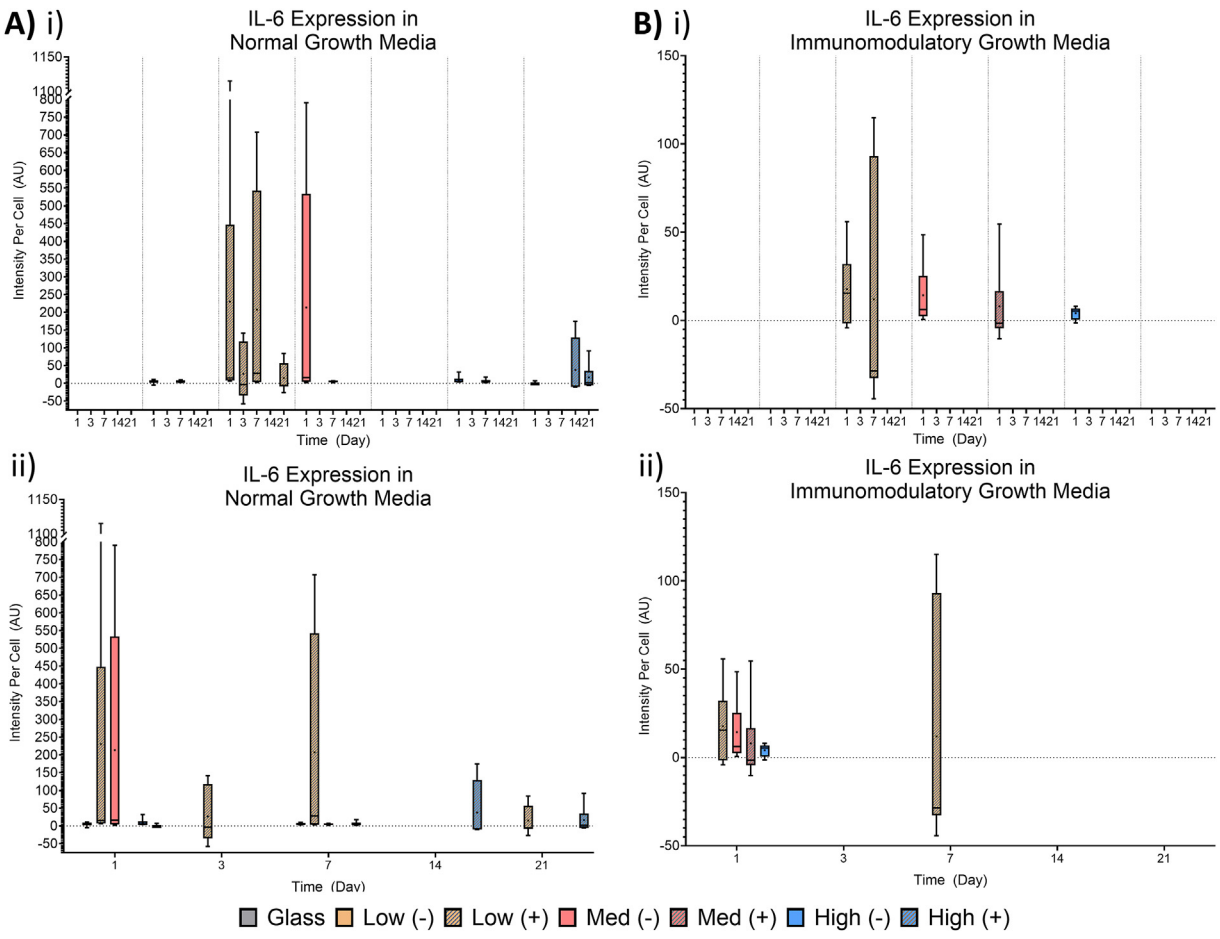

Fig. 5. IL-6 expression over time in A) normal growth media and B) immunomodulatory growth media. i) Data is expressed per gel formulation over time. Data was considered statistically significant for $p < 0.05$ (Note: *$p < 0.05$, **$p < 0.01$, ***$p < 0.001$, ****$p < 0.0001$). ii) Data is expressed at each time point for all gel formulations. Matching letters indicate statistical significance of at least $p < 0.05$.

compared to normal growth media, showing that as the cell recovers from the inflammatory signals and adjusts to the culture conditions, they are able to spread and grow. There does not appear to be an effect of gel type, as this trend occurs for a variety of stiffness gels with and without viscoelastic elements. Supplementary Fig. S5A, which shows the same data over time, corroborates this change in cell area over time. However, the effects of media on aspect ratio was minimal, with only minor differences between cells on control gels and low-stiffness, non-viscoelastic gels at days 3 and 7 (Fig. 4B). Despite the lack of differences between media formulation, Supplementary Fig. S5B demonstrates that aspect ratio increases on all gel types with time; interestingly, our general trend shows a decrease in aspect ratio with increasing stiffness, showing that although there is an increase in area (cell spreading), there is not an increase in elongation.

When evaluating circularity and roundness (Fig. 4C,D and Supplementary Fig. S5CD), we additionally see few differences due to media formulation or gel type; however, for those values that are statistically significant, circularity is typically increased in immunomodulatory growth media conditions, suggesting that there are fewer protrusions in those culture conditions. There is, again, an effect of time, with cells becoming less circular/round over time, suggesting the formation of protrusions over time; this effect is not dependent on gel type. Additionally, there does not appear to be a dependence of viscoelasticity on morphology, as only few samples were found to be statistically significant between non-viscous and viscous gels of the same stiffness, with no discernible trend in gel stiffness or time point.

After day 7, it is more difficult to distinguish any differences in overall cell morphology due to the high confluence on all gel conditions. However, interestingly, in normal growth media, cells on viscoelastic gels at these higher culture days appear to be more aggregated, suggesting increased cell-to-cell contact rather than cell-matrix interactions. To discern if there are any differences in focal adhesion formation due to media or gel conditions, we also investigated vinculin expression over time (Fig. 4E and Supplementary Fig. S5E). While there are differences between cells cultured on glass controls at days 1, 14, and 21 in NGM vs. IGM, there are no additional differences, demonstrating that media composition does not affect focal adhesion formation or quantity. In addition, while many gel conditions show a general trend of increasing vinculin expression over time, this is only statistically significant for gels on glass. Again, there is no discernible effects of the viscoelastic element or gel stiffness on vinculin expression, either.

To summarize, while there are changes to cell area, aspect ratio, circularity, roundness, and to a limited degree vinculin expression over time, these changes occur regardless of gel and media condition. Cell area is predominantly affected by media composition, and the only major trend due to gel stiffness or viscoelasticity is the overall decrease in cellular aspect ratio as the gel stiffness increases. To a limited degree, there is also somewhat of a trend of increasing cell area due to increasing gel stiffness, though this effect is mostly gone by day 7 where the confluence is greater. Therefore, while changes in cytokine expression may be directly related to morphological changes at early time points, specifically differences in cell area and aspect ratio, it is unlikely that morphological differences in the cells and differences between cellular interactions with the different gel conditions are the cause of any cytokine expression differences.

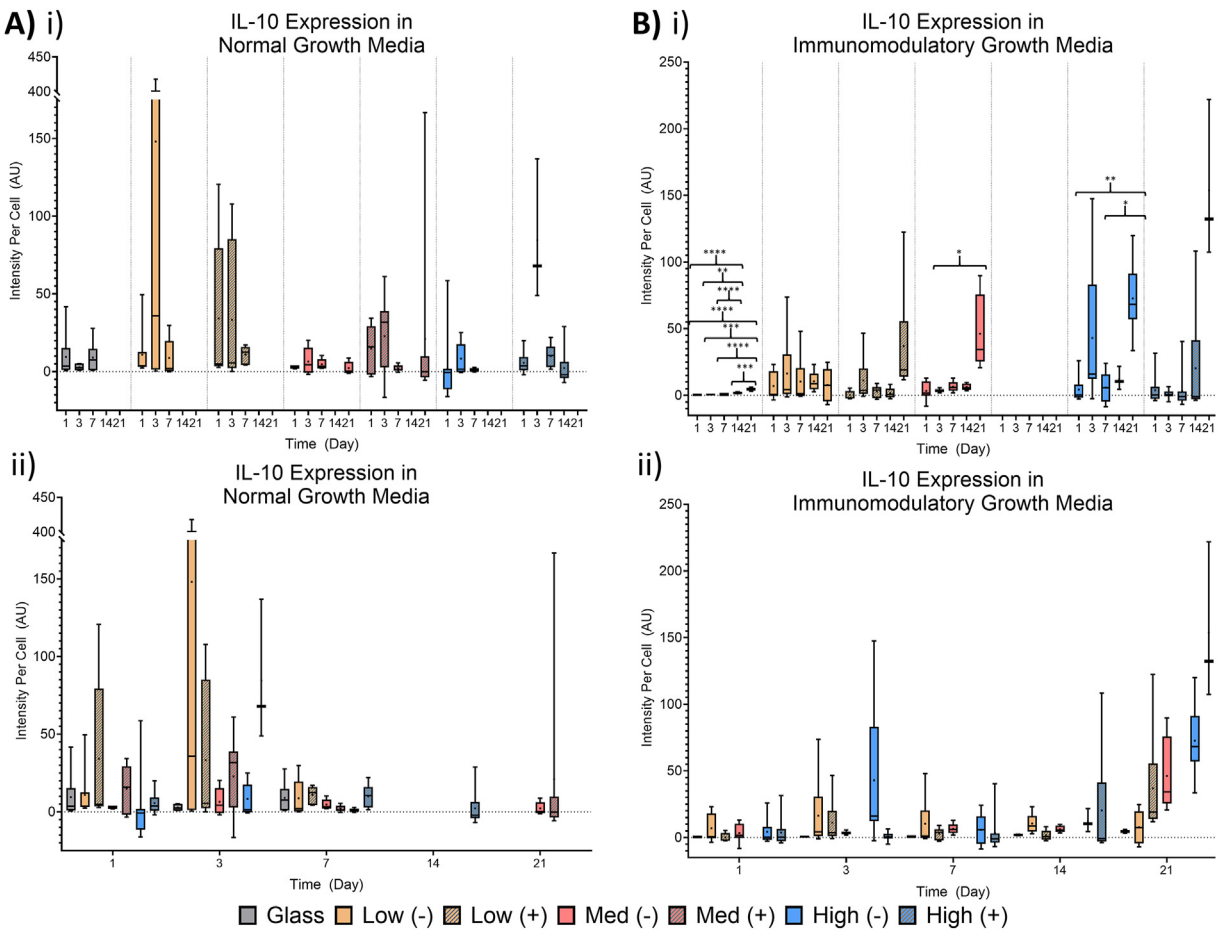

Fig. 6. IL-10 expression over time in A) normal growth media and B) immunomodulatory growth media. i) Data is expressed per gel formulation over time. Data was considered statistically significant for $p < 0.05$ (Note: *$p < 0.05$, **$p < 0.01$, ***$p < 0.001$, ****$p < 0.0001$). ii) Data is expressed at each time point for all gel formulations. Matching letters indicate statistical significance of at least $p < 0.05$.

3.1.2. *Effects of matrix stiffness and viscoelasticity on hMSC immunomodulation*

Since hMSCs are known to have immunomodulatory effects across the entire duration of the wound healing process,[42,43] we sought to investigate a breadth of cytokines that encompasses the roles of hMSCs throughout wound healing. We investigate the intracellular expression of these cytokines at time points relevant to the four phases of wound healing.[44] In normal wounds, healing begins with the hemostasis phase, which emphasizes coagulation and recruitment of immunomodulatory cells. The second phase is the inflammatory phase, which typically takes 1–3 days. This is followed by the proliferation phase, which takes between 3 and 21 days. The fourth and final phase is the remodelling phase, which can take up to 1 year. In particular, we focus on expression of: 1. IL-6, a pro-inflammatory cytokine that we expect to be expressed during the second phase of wound healing;[45] 2. IL-10, an anti-inflammatory cytokine that we expect to be expressed at the transition from phase two to three;[45] 3. PGE_2, a proliferative cytokine that we expect to be expressed during the third phase;[46] and 4. VEGF, an angiogenic cytokine that we expect to occur towards the end of the third phase and throughout the fourth phase.[47] Note that for all graphs, intensity per cell values at or below zero are indicative of no expression beyond baseline background signal; therefore, we are only interested in values above zero indicating a positive intracellular expression. In order to facilitate interpretation of the data, only data for which cytokine expression was above zero is presented; additionally, statistical significance is only shown between conditions for which both conditions have positive cytokine expression above zero. Complete graphs with all data and statistical analysis can be seen in Supplementary Figs. S6–S9. In addition, Supplementary Table S2 lists p-values for all statistically-significant comparisons between conditions in normal growth media vs. immunomodulatory growth media.

In normal growth media, IL-6, an inflammatory cytokine, has positive expression predominantly on low-stiffness, viscoelastic gels; the greatest magnitude of this expression is at lower time points, although it is not statistically significant with time (Fig. 5Ai). There is also some expression at early time points on medium-stiffness, non-viscoelastic gels and some expression at late time points on high- stiffness, non-viscoelastic gels. Low-stiffness and high-stiffness gels without viscoelastic components also have marginal, near-zero, expression at early time points. Despite the lack of immunomodulatory signals, expression of IL-6 is not entirely unexpected as these cells had recently been exposed to passaging and culture on a new environment, supported by the fact that the largest variability between gels at each time point occurs at day 1 (Fig. 5Aii). This is particularly interesting when comparing to the morphology data seen in Figs. 2 and 4, where cell area trends smaller for lower-stiffness gels, and the magnitude of vinculin expression is also lower overall. Therefore, due to the limited cell-matrix interactions and the limited cell-to-cell interactions at these lower time points, the cells are under more stress,[48] likely leading them to express higher levels of the inflammatory cytokine IL-6.

In immunomodulatory media containing inflammatory signals, the variation in IL-6 expression over time is less pronounced. Only minimal IL-6 expression is present in low-stiffness gels with a viscoelastic element at early time points, with some marginal day 1 expression on other gel conditions (Fig. 5Bi). There is also a less pronounced difference between gel types at each time point (Fig. 5Bii). This lack of variability due to

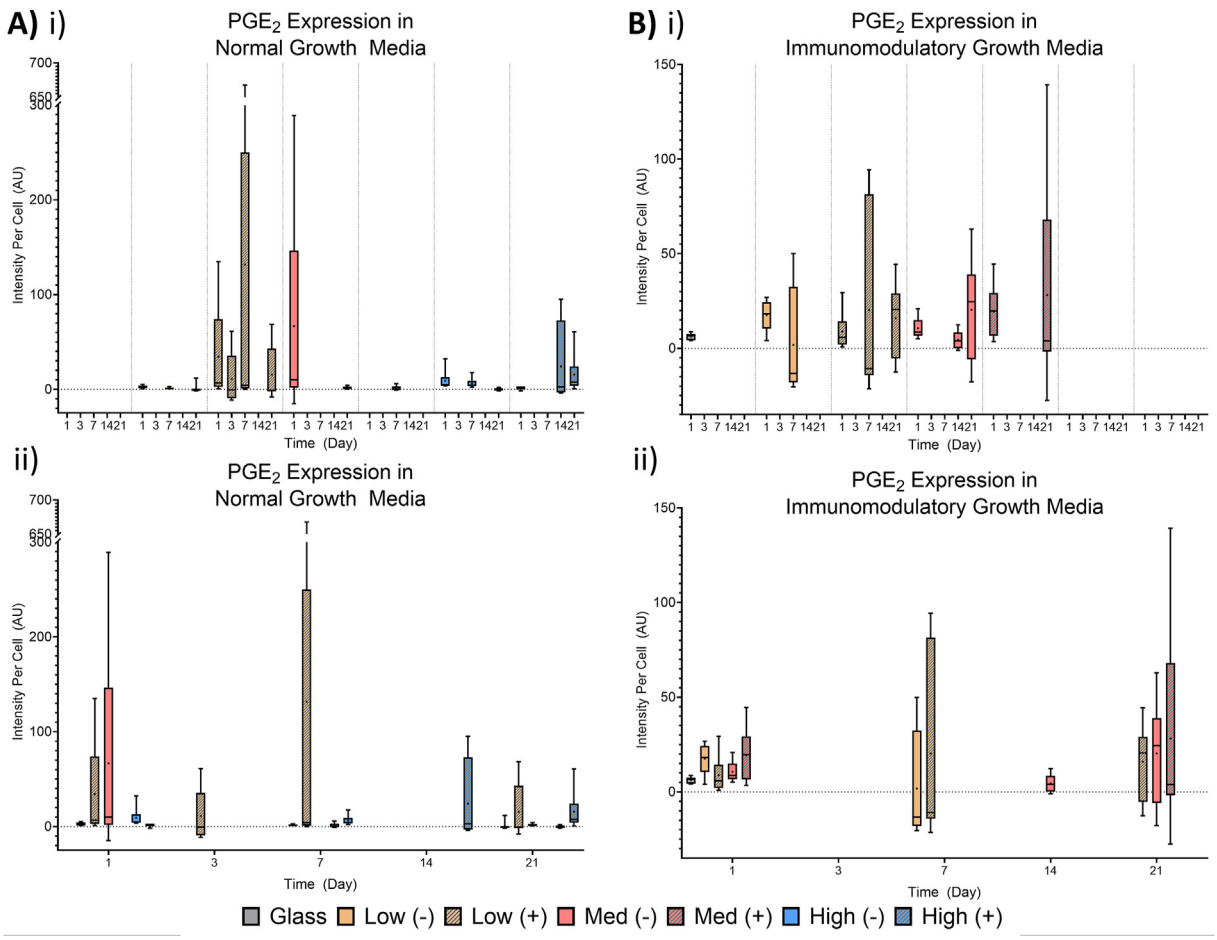

Fig. 7. PGE_2 expression over time in A) normal growth media and B) immunomodulatory growth media. i) Data is expressed per gel formulation over time. Data was considered statistically significant for $p < 0.05$ (Note: *$p < 0.05$, **$p < 0.01$, ***$p < 0.001$, ****$p < 0.0001$). ii) Data is expressed at each time point for all gel formulations. Matching letters indicate statistical significance of at least $p < 0.05$.

matrix stiffness and/or viscoelasticity correlates with the lack of morphological variability (Fig. 4). Notably, although not statistically significant, the greatest range in IL-6 expression in immunomodulatory growth media is for the low-stiffness gels with a viscoelastic element, again consistent with the cell-matrix interactions discussed above.

In comparing the cells in normal growth media vs immunomodulatory growth media, there are some differences. At day 3, low-stiffness, non-viscoelastic gels have statistically decreased expression in immunomodulatory growth media. This is the same for cells on medium-stiffness, non-viscoelastic gels, as well as high-stiffness, non-viscoelastic gels. This trend continues for high-stiffness, non-viscoelastic gels at days 14 and 21, as well. At day 14, cells cultured on a glass substrate also demonstrated statistically decreased IL-6 expression in immunomodulatory growth media, as well as cells on medium-stiffness, viscoelastic and high-stiffness, viscoelastic gels. Finally, at day 21, cells on low-stiffness, non-viscoelastic and medium-stiffness, non-viscoelastic gels also have statistically decreased IL-6 expression in immunomodulatory growth media.

In normal growth media, the greatest IL-10 expression with the least variability is in high-stiffness, viscoelastic gels at day 3 (Fig. 6Ai). This effect is in line with the expected expression of an anti-inflammatory molecule at the transition from the inflammation stage to the proliferation stage of wound healing. Interestingly, there is IL-10 expression in all gel conditions between days 1 and 7, with the greatest magnitude of expression at day 3, although not statistically significant (Fig. 6Aii). This is particularly interesting when compared to the expression of IL-6 in normal growth media (Fig. 5A), which had some expression, albeit minimal, at day 1 for multiple gel conditions, as the IL-10 expression is increasing at the same timeline by which IL-6 expression is decreasing, again in conjunction with the expected timeline of normal wound healing and the cells recovering from passaging and transitioning to metabolic proliferation, shown in Fig. 1.

Culture in an immunomodulatory environment, mimetic of a chronic, non-healing wound wherein the inflammation phase persists, affects this behaviour. The greatest overall response is in the high-stiffness gels, though this time in the non-viscoelastic condition (where cell-matrix interactions dominate), with elevated IL-10 expression at day 21 compared to both days 1 and 7 (Fig. 6Bi). Medium-stiffness, non-viscoelastic gels, as well as the glass controls (indicative of a very high-stiffness, non-viscoelastic condition) also have statistically significant elevated IL-10 expression at day 21 compared to earlier time points. Further, all gel conditions have a trend of increased IL-10 expression at day 21, however it is not statistically significant for any other gel conditions. This suggests that increasing stiffness of the matrix from medium-stiffness to very-high stiffness will eventually encourage the cultured hMSCs to produce anti-inflammatory cytokines, though certainly at a delayed timeline compared to culture in normal growth media. This suggests that increasing the stiffness of the matrix will allow the effects of the chronic, non-healing wound to be overcome, resulting in a transition to the proliferative stage. In this case, there is not a synergistic effect with viscoelasticity, as there is no statistical significance between gel conditions with and without a viscoelastic element, although magnitudes of expression are generally increased on gels with a viscoelastic element this effect was predominant in the gels without a viscoelastic element (Fig. 6Bii).

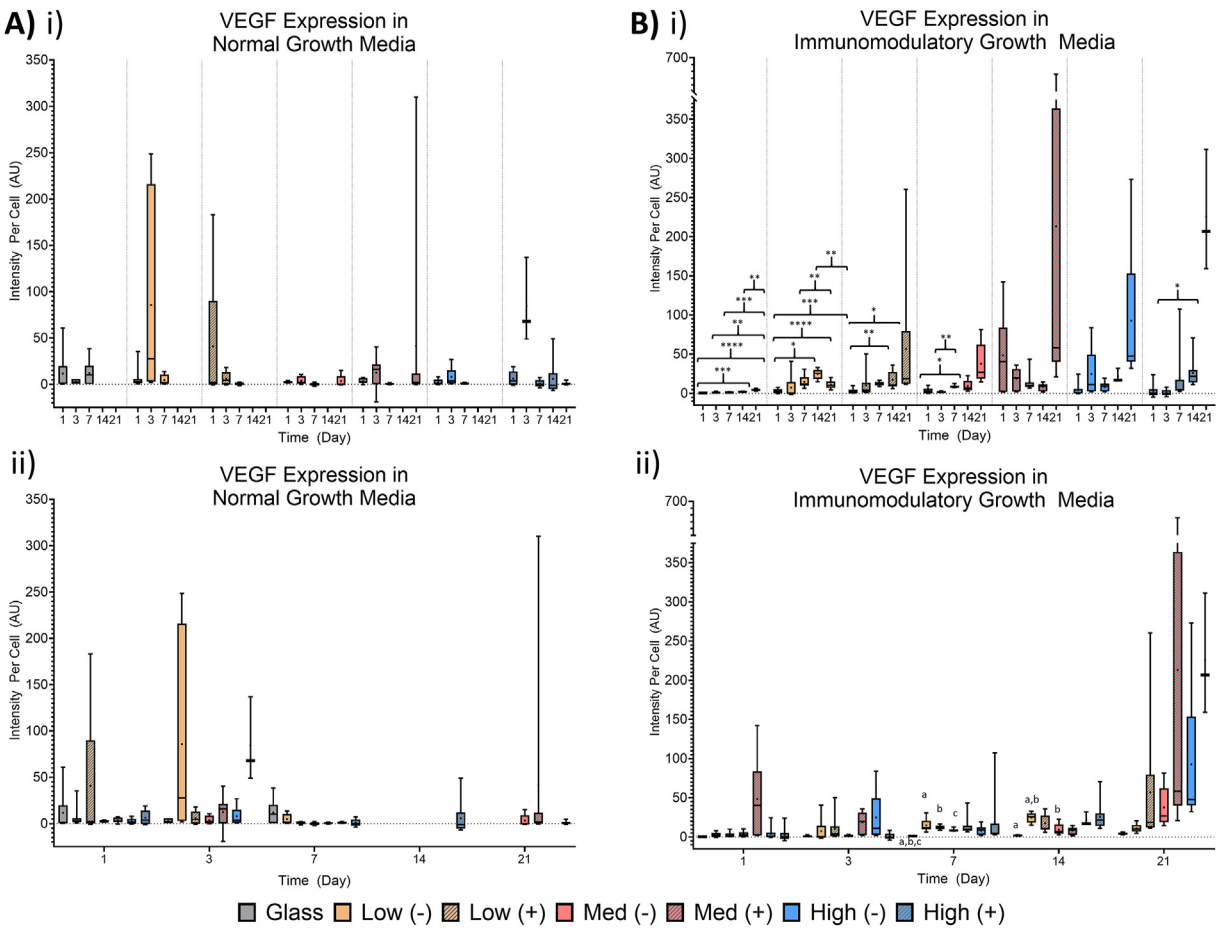

Fig. 8. VEGF expression over time in A) normal growth media and B) immunomodulatory growth media. i) Data is expressed per gel formulation over time. Data was considered statistically significant for $p < 0.05$ (Note: *$p < 0.05$, **$p < 0.01$, ***$p < 0.001$, ****$p < 0.0001$). ii) Data is expressed at each time point for all gel formulations. Matching letters indicate statistical significance of at least $p < 0.05$.

When we compare cells on gels in normal growth media vs immunomodulatory growth media, we find that at days 3, 7, and 14, IL-10 expression is statistically decreased in immunomodulatory media for medium-stiffness, viscoelastic gels. On the other hand, at day 14, cells cultured on glass, low-stiffness, non-viscoelastic gels, and medium-stiffness, non-viscoelastic gels have statistically increased IL-10 expression in immunomodulatory growth media compared to normal growth media; this effect is continued at day 21 for cells cultured on glass, as well as cells cultured on high-stiffness, non-viscoelastic gels. When we compare this to the morphology data that shows larger cell area and decreased aspect ratio for increasing stiffness gels, this suggests that increasing matrix stiffness, and thereby increasing cell spreading and cell-matrix interactions (with increased vinculin at later time points), independent of viscoelasticity, supports a transition to the proliferative stage in inflammatory conditions. In fact, given the decrease in IL-10 expression for cells in immunomodulatory media on medium-stiffness, viscoelastic gels, it is possible that viscoelasticity may negatively impact the effects of the matrix stiffness at these moduli. One interesting note, as well, is that the range of IL-10 expression values for cells in normal growth media is much larger than those cells in immunomodulatory media. This variability is not too surprising when we consider that IL-10, as an anti-inflammatory molecule, is used to stop the inflammation phase and transition to the proliferation phase. In normal growth media, where there are no inflammatory signals present, a greater variation in IL-10 expression would, therefore, not be unexpected.

PGE_2 expression in normal growth media is maximum again on low-stiffness, viscoelastic gels, though the effect is not statistically significant over time due to the large range of data (Fig. 7Ai); however, the greatest magnitude of expression occurs between days 1 and 7 (Fig. 7Aii). Cells on low-stiffness, non-viscoelastic gels, medium-stiffness, non-viscoelastic gels, and high-stiffness gels with or without viscoelasticity do also have changes to PGE_2 expression over time, albeit much lower in magnitude to the PGE_2 expression in the low-stiffness, viscoelastic gels. As mentioned, the greatest expression of PGE_2 is at early-mid time points, which is consistent with the increased proliferation rates seen in Fig. 1A.

Culture of the cells in immunomodulatory media somewhat affects the expression of PGE_2. There is a greater variation in PGE_2 expression for all gel formulations, with days 1, 7, and 21 having the greatest magnitude of expression (Fig. 7Bi). Given the static proliferation rate of cells on all gel formulations beyond day 3 (Fig. 1B), it is likely that the day 1 expression of PGE_2 is partially for the hMSCs themselves (autocrine signalling), whereas expression at the later time points is meant to be immunomodulatory. Indeed, expression of PGE_2 at these time points is consistent with the proliferation phase of wound healing. When comparing between gel formulations, the greatest magnitude of response is seen in the low-stiffness and medium-stiffness gels, with the PGE_2 expression somewhat independent of the incorporation of a viscoelastic element (Fig. 7Bii).

At day 1, expression of PGE_2 is statistically enhanced in immunomodulatory growth media for cells cultured on low-stiffness, non-viscoelastic gels compared to normal growth media. This trend continues at day 3. On day 3, expression of PGE_2 from cells cultured on high-stiffness, non-viscoelastic gels in immunomodulatory growth media is decreased compared to normal growth media, a trend which continues at day 7, supporting the results described previously indicating that lower to medium-stiffness gels enhance PGE_2 expression. Day 7 also sees this same trend for cells on glass and high-stiffness, viscoelastic gels, further supporting this conclusion. Days 14 and 21 continue this decreased

expression of PGE_2 in immunomodulatory growth media compared to normal growth media for cells cultured on glass, indicative of a very-high stiffness condition.

VEGF is a cytokine known to influence angiogenesis. In the normal wound healing process, this is common in the proliferation phases from days 3–21 and the remodelling phase from days 21+.[49] In normal growth media, which would mimic the non-inflammatory conditions present at these stages in normal wound healing, there does not appear to be any consistent effects, aside from increased positive expression of VEGF on days 1–7 as opposed to days 14 and 21 (Fig. 8Ai). This is consistent with the proliferation phase of the normal wound healing process. In addition, there is no statistical difference between gel conditions at any time point, although magnitudes of response do trend larger for lower-stiffness gels, independent of a viscoelastic element (Fig. 8Aii).

In immunomodulatory media containing inflammatory signals, these trends appear to reverse. In general, regardless of matrix stiffness and viscoelasticity, VEGF expression increases over time, with maximum VEGF expression at days 14 and 21 (Fig. 8Bi). Although chronic, non-healing wounds are classified by their inability to move beyond the inflammation phase and heal, it appears that culture of the cells on varying matrix stiffness and viscoelasticity conditions improves VEGF expression despite the chronic inflammatory signals. Specifically, at day 7, VEGF expression is maximum for cells on low-stiffness, non-viscoelastic gels, low-stiffness, viscoelastic gels, and medium-stiffness, non-viscoelastic gels all compared to glass controls (Fig. 8Bii). At day 14, this trend continues, with the expression of VEGF on low-stiffness, non-viscoelastic gels being the greatest. Therefore, culture on lower-stiffness gels, independent of viscoelasticity, leads to increased VEGF expression in inflammatory conditions. This effect is particularly interesting when considering it in regard to IL-10 expression, which is statistically increased on these gels in immunomodulatory growth media compared to normal growth media at this same time point. This suggests that the cells releasing the anti-inflammatory cytokines can modulate the environment enough to also promote release of an angiogenic cytokine when cultured on low-stiffness, non-viscoelastic gels.

Interestingly, VEGF expression is consistently greater on cells cultured in immunomodulatory growth media compared to normal growth media. At day 7, this effect is statistically significant for low-stiffness, viscoelastic gels and medium-stiffness, non-viscoelastic gels. At day 14, this effect is statistically significant for glass, low-stiffness gels independent of viscoelasticity, and medium-stiffness, viscoelastic gels. At day 21, this effect continues for glass and low-stiffness, non-viscoelastic gels. This suggests that the presence of the inflammatory signals, whether or not they are being modulated by expression of IL-10, stimulates VEGF expression, essentially 'telling' the cells that healing is needed. In the normal growth media condition, the cells were never exposed to a wound-like environment, so they never received the signal that healing was needed. Even though there was VEGF expression at low time points in normal growth media, this is further supported by the fact that the range of VEGF expression at those time points was very large, demonstrating the large variability in VEGF expression (Fig. 8Aii).

4. Conclusions

Despite the interesting conclusions that suggest the interplay between matrix stiffness and viscoelasticity effects on hMSC immunomodulatory behavior, there are several limitations of the study to be considered. First, this study only considers intracellular expression/production of the cytokines through the use of immunocytochemistry and, as such, does not evaluate extracellular production or gene expression. In addition, this study considers normal growth media, mimetic of a non-wound environment, and immunomodulatory growth media containing inflammatory signals, mimetic of a chronic, non-healing wound environment. It would also be interesting to evaluate a third condition, where the hMSCs are exposed to inflammatory signals for 1–3 days before transitioning to normal growth media for days 3–21, following the stages of normal wound healing. Future studies will consider these effects.

However, regardless of the study's limitations, the conclusions of the study are rather exciting. There are clear effects of matrix stiffness and viscoelasticity on cytokine expression, sometimes synergistic and sometimes unilateral, and these effects are further influenced by biochemical signalling, either attenuating or increasing the response. It is also clear from this broad study that there is no one stiffness/viscoelasticity combination that is ideal for all immunomodulatory applications. Expression of the inflammatory cytokine IL-6 is predominant on low-stiffness, viscoelastic gels. On the other hand, IL-10 expression is most affected by higher-stiffness gels, with potentially inhibitory effects when viscoelastic elements are added. PGE_2 expression is enhanced on low-stiffness and, to some degree, medium-stiffness gels, with potentially a synergistic effect of viscoelasticity depending on the biochemical signaling. Finally, VEGF expression is predominant on lower stiffness gels, somewhat independent of viscoelasticity. In general, all of these cytokines have increased expression in immunomodulatory growth media over normal growth media, demonstrating that the biochemical signalling indicating a 'wound' is necessary for activation of hMSC immunomodulatory effects. The sole exception is expression of the inflammatory cytokine IL-6, which is greatest in normal growth media. It is possible that the presence of the other inflammatory molecules already present in the immunomodulatory growth media is sufficient to affect the role of the hMSCs from informing the surrounding environment of a 'wound' to predominantly focusing on 'healing' effects. The results of this study therefore provide a broad perspective on the immunomodulatory behaviour of hMSCs and how these are affected by matrix stiffness and viscoelasticity. In general, most immunomodulatory behaviors of hMSCs are enhanced on low-stiffness matrices, however this is the most valid in treatment of wounds following normal wound healing. In chronic, non-healing wounds that are incapable of escaping the inflammatory state, a high-stiffness matrix to increase expression of IL-10 may be more valuable. In addition, viscoelasticity has both inhibitory and accentuating effects, based on the cytokine. Therefore, future studies may utilize the information in this study to select the matrix stiffness/viscoelasticity condition that is most valuable for their chosen application. In addition, this study demonstrates that hMSC immunomodulatory behaviour, not just cell-matrix interactions and differentiation, are invariably affected by matrix stiffness and viscoelasticity, and the presence of inflammatory signals in the IGM can have significant effects on changes to cell area; our current work is focused on understanding the pathways by which matrix stiffness and viscoelasticity affect these immunomodulatory responses, whether through mechanotransduction pathways or otherwise.

CRediT authorship contribution statement

Sara J. Olsen: Writing – review & editing, Writing – original draft, Visualization, Validation, Project administration, Methodology, Investigation, Formal analysis, Data curation. **Rose E. Leader:** Writing – original draft, Visualization, Validation, Investigation, Formal analysis. **Abigail L. Mortimer:** Investigation. **Bethany Almeida:** Writing – review & editing, Writing – original draft, Visualization, Supervision, Software, Resources, Project administration, Funding acquisition, Formal analysis, Data curation, Conceptualization.

Availability of data and materials

All data generated or analyzed during the current study are included in this published article and its supplementary information files. The datasets used and/or analyzed during the current study are available from the corresponding author on reasonable request.

Ethical approval

This study does not contain any studies with human or animal subjects performed by any of the authors.

Declaration of Generative AI and AI-assisted technologies in the writing process

No generative AI was used in any aspect of this manuscript.

Funding

The authors acknowledge funding from Clarkson University.

Declaration of competing interest

The authors declare that they have no known competing financial interests or personal relationships that could have appeared to influence the work reported in this paper.

Acknowledgements

We would like to acknowledge Hubert Bilan from the Center for Advanced Materials Processing (CAMP) Biomaterials Lab for support with DMA and Rheology, Reilly Avila for help with occasional feeding of cells, and Rabia Fatima for help with staining procedures. In addition, we would like to acknowledge funding from Clarkson University.

Appendix A. Supplementary data

Supplementary data to this article can be found online at https://doi.org/10.1016/j.mbm.2024.100111.

References

1. Pittenger MF, Mackay AM, Beck SC, et al. Multilineage potential of adult human mesenchymal stem cells. *Science (1979)*. 1999;284:143–147. https://doi.org/10.1126/science.284.5411.143.
2. Maxson S, Lopez EA, Yoo D, Danilkovitch-Miagkova A, Leroux MA. Concise review: role of mesenchymal stem cells in wound repair. *Stem Cells Transl Med*. 2012;1:142–149. https://doi.org/10.5966/sctm.2011-0018.
3. Haddad R, Saldanha-Araujo F. Mechanisms of T-cell immunosuppression by mesenchymal stromal cells: what do we know so far? *BioMed Res Int*. 2014;2014:216806. https://doi.org/10.1155/2014/216806.
4. Laing AG, Fanelli G, Ramirez-Valdez A, Lechler RI, Lombardi G, Sharpe PT. Mesenchymal stem cells inhibit T-cell function through conserved induction of cellular stress. *PLoS One*. 2019;14:e0213170. https://doi.org/10.1371/journal.pone.0213170.
5. Duffy MM, Ritter T, Ceredig R, Griffin MD. Mesenchymal stem cell effects on T-cell effector pathways. *Stem Cell Res Ther*. 2011;2:34. https://doi.org/10.1186/scrt75.
6. Ayavoo T, Murugesan K, Gnanasekaran A. Roles and mechanisms of stem cell in wound healing. *Stem Cell Investig*. 2021;8:4. https://doi.org/10.21037/sci-2020-027, 4.
7. Ren G, Zhang L, Zhao X, et al. Mesenchymal stem cell-mediated immunosuppression occurs via concerted action of chemokines and nitric oxide. *Cell Stem Cell*. 2008;2:141–150. https://doi.org/10.1016/j.stem.2007.11.014.
8. Aggarwal S, Pittenger MF. Human mesenchymal stem cells modulate allogeneic immune cell responses. *Blood*. 2005;105:1815–1822. https://doi.org/10.1182/blood-2004-04-1559.
9. Han G, Ceilley R. Chronic wound healing: a review of current management and treatments. *Adv Ther*. 2017;34:599–610. https://doi.org/10.1007/s12325-017-0478-y.
10. Järbrink K, Ni G, Sönnergren H, et al. Prevalence and incidence of chronic wounds and related complications: a protocol for a systematic review. *Syst Rev*. 2016;5:152. https://doi.org/10.1186/s13643-016-0329-y.
11. Im G-B, Kim YH, Kim Y-J, et al. Enhancing the wound healing effect of conditioned medium collected from mesenchymal stem cells with high passage number using bioreducible nanoparticles. *Int J Mol Sci*. 2019;20:4835. https://doi.org/10.3390/ijms20194835.
12. Kim HJ, Park J-S. Usage of human mesenchymal stem cells in cell-based therapy: advantages and disadvantages. *Dev Reprod*. 2017;21:1–10. https://doi.org/10.12717/DR.2017.21.1.001.
13. Noronha N de C, Mizukami A, Caliári-Oliveira C, et al. Priming approaches to improve the efficacy of mesenchymal stromal cell-based therapies. *Stem Cell Res Ther*. 2019;10:131. https://doi.org/10.1186/s13287-019-1224-y.
14. Gao F, Chiu SM, Motan DAL, et al. Mesenchymal stem cells and immunomodulation: current status and future prospects. *Cell Death Dis*. 2016;7:e2062. https://doi.org/10.1038/cddis.2015.327. e2062.
15. Gomez-Salazar M, Gonzalez-Galofre ZN, Casamitjana J, Crisan M, James AW, Péault B. Five decades later, are mesenchymal stem cells still relevant? *Front Bioeng Biotechnol*. 2020;8:148. https://www.frontiersin.org/article/10.3389/fbioe.2020.00148.
16. Pittenger MF, Discher DE, Péault BM, Phinney DG, Hare JM, Caplan AI. Mesenchymal stem cell perspective: cell biology to clinical progress. *NPJ Regen Med*. 2019;4:22. https://doi.org/10.1038/s41536-019-0083-6.
17. Dunn CM, Kameishi S, Grainger DW, Okano T. Strategies to address mesenchymal stem/stromal cell heterogeneity in immunomodulatory profiles to improve cell-based therapies. *Acta Biomater*. 2021;133:114–125. https://doi.org/10.1016/j.actbio.2021.03.069.
18. Li J, Wu Z, Zhao L, et al. The heterogeneity of mesenchymal stem cells: an important issue to be addressed in cell therapy. *Stem Cell Res Ther*. 2023;14:381. https://doi.org/10.1186/s13287-023-03587-y.
19. Yang C, Tibbitt MW, Basta L, Anseth KS. Mechanical memory and dosing influence stem cell fate. *Nat Mater*. 2014;13:645–652. https://doi.org/10.1038/nmat3889.
20. Li B, Moshfegh C, Lin Z, Albuschies J, Vogel V. Mesenchymal stem cells exploit extracellular matrix as mechanotransducer. *Sci Rep*. 2013;3:2425. https://doi.org/10.1038/srep02425.
21. Killaars AR, Walker CJ, Anseth KS. Nuclear mechanosensing controls MSC osteogenic potential through HDAC epigenetic remodeling. *Proc Natl Acad Sci USA*. 2020;117:21258–21266. https://doi.org/10.1073/pnas.2006765117.
22. Loebel C, Mauck RL, Burdick JA. Local nascent protein deposition and remodelling guide mesenchymal stromal cell mechanosensing and fate in three-dimensional hydrogels. *Nat Mater*. 2019;18:883–891. https://doi.org/10.1038/s41563-019-0307-6.
23. Engler AJ, Sen S, Sweeney HL, Discher DE. Matrix elasticity directs stem cell lineage specification. *Cell*. 2006;126:677–689. https://doi.org/10.1016/j.cell.2006.06.044.
24. Chaudhuri O, Cooper-White J, Janmey PA, Mooney DJ, Shenoy VB. Effects of extracellular matrix viscoelasticity on cellular behaviour. *Nature*. 2020;584:535–546. https://doi.org/10.1038/s41586-020-2612-2.
25. Chaudhuri O, Gu L, Klumpers D, et al. Hydrogels with tunable stress relaxation regulate stem cell fate and activity. *Nat Mater*. 2016;15:326–334. https://doi.org/10.1038/nmat4489.
26. Cantini M, Donnelly H, Dalby MJ, Salmeron-Sanchez M. The plot thickens: the emerging role of matrix viscosity in cell mechanotransduction. *Adv Healthc Mater*. 2020;9. https://doi.org/10.1002/adhm.201901259.
27. Ahearne M. Introduction to cell–hydrogel mechanosensing. *Interface Focus*. 2014;4:20130038. https://doi.org/10.1098/rsfs.2013.0038.
28. Li J, Liu Y, Zhang Y, et al. Biophysical and biochemical cues of biomaterials guide mesenchymal stem cell behaviors. *Front Cell Dev Biol*. 2021;9. https://doi.org/10.3389/fcell.2021.640388.
29. Brennan MÁ, Layrolle P, Mooney DJ. Biomaterials functionalized with MSC secreted extracellular vesicles and soluble factors for tissue regeneration. *Adv Funct Mater*. 2020;30. https://doi.org/10.1002/adfm.201909125.
30. Keshavarz R, Olsen S, Almeida B. Using biomaterials to improve mesenchymal stem cell therapies for chronic, nonhealing wounds. *Bioeng Transl Med*. 2024;9. https://doi.org/10.1002/btm2.10598.
31. Phuagkhaopong S, Mendes L, Müller K, et al. Silk hydrogel substrate stress relaxation primes mesenchymal stem cell behavior in 2D. *ACS Appl Mater Interfaces*. 2021;13:30420–30433. https://doi.org/10.1021/acsami.1c09071.
32. Liu FD, Pishesha N, Poon Z, Kaushik T, Van Vliet KJ. Material viscoelastic properties modulate the mesenchymal stem cell secretome for applications in hematopoietic recovery. *ACS Biomater Sci Eng*. 2017;3:3292–3306. https://doi.org/10.1021/acsbiomaterials.7b00644.
33. Wan WS, Stephen L, H CM, J MD, Jae-Won S. Soft extracellular matrix enhances inflammatory activation of mesenchymal stromal cells to induce monocyte production and trafficking. *Sci Adv*. 2021;6. https://doi.org/10.1126/sciadv.aaw0158. eaaw0158.
34. Lee HJ, Diaz MF, Ewere A, Olson SD, Cox Jr CS, Wenzel PL. Focal adhesion kinase signaling regulates anti-inflammatory function of bone marrow mesenchymal stromal cells induced by biomechanical force. *Cell Signal*. 2017;38:1–9. https://doi.org/10.1016/j.cellsig.2017.06.012.
35. Gonzalez-Pujana A, de Lázaro I, Vining KH, et al. 3D encapsulation and inflammatory licensing of mesenchymal stromal cells alter the expression of common reference genes used in real-time RT-qPCR. *Biomater Sci*. 2020;8:6741–6753. https://doi.org/10.1039/D0BM01562H.
36. Tse JR, Engler AJ. Preparation of hydrogel substrates with tunable mechanical properties. *Curr Protoc Cell Biol*. 2010;47. https://doi.org/10.1002/0471143030.cb1016s47.
37. Pogoda K, Charrier E, Janmey P. A novel method to make polyacrylamide gels with mechanical properties resembling those of biological tissues. *Bio Protoc*. 2021;11. https://doi.org/10.21769/BioProtoc.4131.
38. Charrier EE, Pogoda K, Wells RG, Janmey PA. Control of cell morphology and differentiation by substrates with independently tunable elasticity and viscous dissipation. *Nat Commun*. 2018;9:449. https://doi.org/10.1038/s41467-018-02906-9.
39. Jin P, Zhao Y, Liu H, et al. Interferon-γ and tumor necrosis factor-α polarize bone marrow stromal cells uniformly to a Th1 phenotype. *Sci Rep*. 2016;6:26345. https://doi.org/10.1038/srep26345.
40. Lv H, Li L, Sun M, et al. Mechanism of regulation of stem cell differentiation by matrix stiffness. *Stem Cell Res Ther*. 2015;6:103. https://doi.org/10.1186/s13287-015-0083-4.
41. Kilian KA, Bugarija B, Lahn BT, Mrksich M. Geometric cues for directing the differentiation of mesenchymal stem cells. *Proc Natl Acad Sci USA*. 2010;107:4872–4877. https://doi.org/10.1073/pnas.0903269107.
42. Song N, Scholtemeijer M, Shah K. Mesenchymal stem cell immunomodulation: mechanisms and therapeutic potential. *Trends Pharmacol Sci*. 2020;41:653–664. https://doi.org/10.1016/j.tips.2020.06.009.

43. Seo BF, Jung S-N. The immunomodulatory effects of mesenchymal stem cells in prevention or treatment of excessive scars. *Stem Cells Int*. 2016;2016. https://doi.org/10.1155/2016/6937976.
44. Rodrigues M, Kosaric N, Bonham CA, Gurtner GC. Wound healing: a cellular perspective. *Physiol Rev*. 2019;99:665–706. https://doi.org/10.1152/physrev.00067.2017.
45. Mahmoud NN, Hamad K, Al Shibitini A, et al. Investigating inflammatory markers in wound healing: understanding implications and identifying artifacts. *ACS Pharmacol Transl Sci*. 2024;7:18–27. https://doi.org/10.1021/acsptsci.3c00336.
46. Sandulache VC, Parekh A, Li-Korotky H, Dohar JE, Hebda PA. Prostaglandin E2 differentially modulates human fetal and adult dermal fibroblast migration and contraction: implication for wound healing. *Wound Repair Regen*. 2006;14:633–643. https://doi.org/10.1111/j.1743-6109.2006.00156.x.
47. Tonnesen MG, Feng X, Clark RAF. Angiogenesis in wound healing. *J Invest Dermatol Symp Proc*. 2000;5:40–46. https://doi.org/10.1046/j.1087-0024.2000.00014.x.
48. Hu Q, Xia X, Kang X, et al. A review of physiological and cellular mechanisms underlying fibrotic postoperative adhesion. *Int J Biol Sci*. 2021;17:298–306. https://doi.org/10.7150/ijbs.54403.
49. Strodtbeck F. Physiology of wound healing. *Newborn Infant Nurs Rev*. 2001;1:43–52. https://doi.org/10.1053/nbin.2001.23176.